

# THEORETICAL AND EXPERIMENTAL INVESTIGATIONS ON CHOKING PHENOMENA OF AXISYMMETRIC CONVERGENT NOZZLE FLOW

**Ryuta ISOZUMI\*, Kazunori KUBO\*, Daisuke ONO\*, and Yoshiaki MIYAZATO\***

**\*Department of Mechanical Systems Engineering, The University of Kitakyushu**  
*miyazato@kitakyu-u.ac.jp*

**Keywords:** *compressible flow, choking, flow model, convergent nozzle*

## Abstract

*Choking phenomena of compressible flows through an axisymmetric convergent nozzle have been theoretically and experimentally explored. Choking criteria of a convergent nozzle flow are proposed from experiment and theory. A nozzle of a variable length from the inlet to exit has been used for the purpose of the boundary layer development on the nozzle wall. Pitot probe surveys at the nozzle exit plane as well as static pressure measurements along the nozzle wall have been performed. The experimental results of the choking pressure ratio and freestream Mach numbers at the nozzle exit plane when nozzle flow is just choked are compared with those calculated by the flow model proposed. The present analytical values are in good quantitative agreement with the experimental results.*

## 1 Introduction

When one-dimensional isentropic flow through a convergent nozzle is accelerated by a reduction in back pressure with certain fixed stagnation states at the upstream the flow velocity at the nozzle exit plane increases monotonically until the velocity of sound is reached at the exit plane. The ratio of back pressure to upstream stagnation pressure at which sonic velocity occurs at the nozzle exit plane is called the critical pressure ratio. After the critical pressure ratio is attained, the entire

flow characteristics in the nozzle upstream of the exit plane are kept constant regardless of any further decrease in back pressure. This phenomenon is known as the flow choking<sup>[1]</sup>. When the flow is choked the mass flow rate depends only on the stagnation conditions upstream of the nozzle and remains constant for all back pressures below the critical pressure. Therefore, when convergent nozzles or convergent-divergent nozzles are used to measure mass flow rates as flow-metering devices based on the choking phenomena, they are called critical nozzles.

Guidelines concerning critical nozzles have been covered by the ISO Standard 9300<sup>[2]</sup>. This standard is valid only for critical nozzles with the theoretical Reynolds numbers from  $10^5$  to  $10^7$ . Therefore, when critical nozzles are applied to a measurement in mass flow rates at low Reynolds numbers, there is a further problem which needs to be solved. The experiments with a quadrant nozzle of Nakao and Takamoto<sup>[3]</sup> showed that in ranges of the throat Reynolds numbers less than around 30,000 the choking pressure ratio is always lower than the theoretical one not taking boundary layers into consideration and the experimental critical pressure ratio decreases as the throat Reynolds number decreases.

The theory of the steady one-dimensional isentropic flow of a perfect gas with a specific heat ratio of 1.4 through a convergent nozzle shows the choking pressure ratio of 0.528. In this theoretical analysis the

velocity profile at the nozzle exit plane is assumed to be constant over the cross section of the nozzle. As reported in the experiments of Nakao and Takamoto [3] the critical pressure ratio is always smaller than the theoretical one. Because the actual flow has the nonuniform velocity distribution caused by the boundary layer developing along the nozzle wall. In the present circumstances, however, a relationship between boundary layer and choking phenomenon remains to be fully elucidated.

From the practical engineering viewpoint, it is important to know choking criteria such as the choking pressure ratio, critical mass flow rate, and critical Mach numbers. This requires a straightforward, simple flow model based upon the physics of choked flow rather than the numerical computations using full Navier-Stokes equations. Several flow models to predict choking criteria have been developed so far. For example, Bernstein, Heiser, and Hevenor [4] presented a simple flow model based upon the compound compressible nozzle flow theory made by Pearson, Holliday, and Smith [5]. It was assumed in their flow model that the flow in each stream is steady, adiabatic, and isentropic and that each fluid is a perfect gas with constant thermodynamic properties but mixing effects are excluded. Using the assumptions above, they analyzed the behavior of one or more gas streams flowing through a single convergent divergent nozzle and showed that the compound-compressible flow is choked at the nozzle throat, although the individual stream Mach numbers there are not equal to unity.

However, little attention has been given to effects of the boundary layer thickness on the choking phenomenon of a convergent nozzle flow. Therefore, the aim of the present study is to clarify choking phenomena of convergent nozzles taking boundary layers into account. Experiments of compressible flow through an axisymmetric convergent nozzle have been carried out to investigate the flow choking phenomena. Also, a flow model is proposed to calculate choking criteria. The experimental results of the choking pressure ratio and freestream Mach numbers at the nozzle exit plane when nozzle flow is just choked are

compared with those calculated by the present flow model. Based upon these comparisons, the mechanism of the choking of the flow with the non-uniform velocity distribution by the influence of the boundary layers is made clear.

## 2 Theoretical Analysis

### 2.1 Mass-Averaging Technique

Generally, the velocity or density in compressible viscous duct flows is not uniform over the duct cross-sectional area. Some assumptions are very frequently made concerning the proper averaging concept to tackle the flow one-dimensionally. Usual averaging techniques require very complicated equations on the conservations of mass, momentum, and energy. However, their complexities can be avoided by the mass-averaging techniques [6].

The mass-averaged flow properties will be defined as  $\bar{u}$ ,  $\bar{a}$ , and  $\bar{T}$ :

$$\bar{u} \equiv \left( \frac{\int \rho u^3 dA}{\int \rho u dA} \right)^{1/2} \quad (1)$$

$$\bar{a} \equiv \left( \frac{\int a^2 \rho u dA}{\int \rho u dA} \right)^{1/2} \quad (2)$$

$$\bar{T} \equiv \frac{\int T \rho u dA}{\int \rho u dA} \quad (3)$$

where  $u$  is the local velocity,  $a$  the local speed of sound,  $T$  the local temperature,  $A$  the cross-sectional area of the duct, and  $\rho$  the local density.

The mass-weighted averaging density is given by

$$\bar{\rho} \equiv \frac{\int \rho u dA}{\int u dA} \quad (4)$$

Using these averaged properties, the equation of state, isentropic relation and energy equation can be written without requiring correction factors for the conservations of mass,

momentum and energy. Here, two shape factors are defined as follows:

$$\sigma \equiv \frac{\bar{\rho}\bar{u}A}{\int \rho u dA} \quad (5)$$

$$\xi \equiv \frac{\int \rho u^2 dA}{\bar{u} \int \rho u dA} \quad (6)$$

As seen in general textbooks, the products  $\sigma\xi$  and  $\sigma^2$  indicate the momentum and kinetic energy correction factors respectively.

$$\int \rho u dA = \frac{\bar{\rho}\bar{u}A}{\sigma} \quad (7)$$

$$\int \rho u^2 dA = \frac{\xi}{\sigma} \bar{\rho}\bar{u}^2 A \quad (8)$$

## 2.2 Conservation Laws across Weak Normal Shock Wave

Compressible fluids through a constant area duct with a diameter of  $D$  are considered for the present analysis. The conservation relations for mass, momentum, and energy can be written for a control volume enclosing a weak normal shock wave as shown by dashed lines in Fig.1. The wall friction is assumed to be negligible between sections 1 and 2, i.e. upstream and downstream of a normal shock, as shown in Fig.1.

For a steady one-dimensional flow, the equations of conservation are

$$\int \rho_1 u_1 dA = \int \rho_2 u_2 dA \quad (9)$$

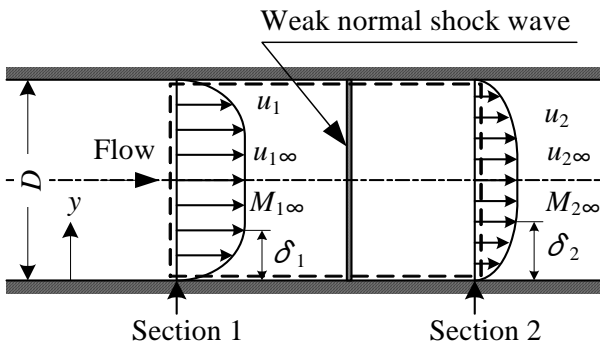


**Figure 1. Control volume enclosing weak normal shock wave**

$$\int (p_1 + \rho_1 u_1^2) dA = \int (p_2 + \rho_2 u_2^2) dA \quad (10)$$

$$\int \left( C_p T_1 + \frac{u_1^2}{2} \right) \rho_1 u_1 dA = \int \left( C_p T_2 + \frac{u_2^2}{2} \right) \rho_2 u_2 dA \quad (11)$$

where subscripts 1 and 2 refer to the states at sections 1 and 2, respectively.

The state equation for a perfect gas with  $\gamma = 1.4$  is given by

$$p = \rho RT \quad (12)$$

For the turbulent boundary layer, the power law velocity profile is assumed by

$$\frac{u}{u_\infty} = \left( \frac{y}{\delta} \right)^{1/n} \quad (0 \leq y \leq \delta) \quad (13)$$

with  $u = u_\infty$  for  $\delta < y < D/2$  where  $y$  is the normal distance from the duct wall.

From assumptions of constant pressure and total temperature, as described in usual boundary layer theory, the density ratio inside and at the edge of the boundary layer is obtained:

$$\frac{\rho}{\rho_e} = \frac{1}{1 + \frac{\gamma-1}{2} M_\infty^2 \left[ 1 - \left( \frac{u}{u_\infty} \right)^2 \right]} \quad (14)$$

where  $M_\infty$  is  $u_\infty / a_\infty$ .

## 2.3 Relations across Weak Normal Shock

Using the relations given in Eqs.(1)~(4), (7), and (8), Eqs. (9)~(11) can be arranged to give

$$\frac{\bar{\rho}_1 \bar{u}_1}{\sigma_1} = \frac{\bar{\rho}_2 \bar{u}_2}{\sigma_2} \quad (15)$$

$$p_1 + \frac{\xi_1}{\sigma_1} \bar{\rho}_1 \bar{u}_1^2 = p_2 + \frac{\xi_2}{\sigma_2} \bar{\rho}_2 \bar{u}_2^2 \quad (16)$$

$$\gamma \frac{p_1}{\bar{\rho}_1} + \frac{\gamma-1}{2} \bar{u}_1^2 = \gamma \frac{p_2}{\bar{\rho}_2} + \frac{\gamma-1}{2} \bar{u}_2^2 \quad (17)$$

When the flow is uniform, the shape factors are unity and the overbars may be omitted from Eqs. (1)~(4) and (15)~(17), which then reduce to the usual one-dimensional forms. These equations form the basis of the classical normal shock relations.

An elegant method of solving the integral relations for nonuniform flow is obtained by transforming them to the conventional one-dimensional forms through absorbing the known shape factors into the variables and constants<sup>[7]</sup>. Here the variables

with the carets are introduced for the simplicity for the analysis later and are related to the mass averaged variables as follows:

$$\hat{u} \equiv \bar{u}, \quad \hat{\rho} \equiv \bar{\rho}, \quad \hat{p} \equiv \frac{\sigma}{\xi} p, \quad \hat{T} \equiv \bar{T}, \quad \hat{R} \equiv \frac{\sigma}{\xi} R, \\ \frac{\hat{\gamma}-1}{\hat{\gamma}} \equiv \frac{\sigma}{\xi} \frac{\gamma-1}{\gamma}, \quad \hat{a}^2 \equiv \tilde{\gamma} \frac{\hat{p}}{\hat{\rho}}, \quad \hat{M} \equiv \frac{\hat{u}}{\hat{a}} \quad (18)$$

The manipulations can be somewhat simplified by the introduction of a new shape factor  $\phi$ , defined as

$$\phi \equiv \frac{1}{\sqrt{\frac{\xi}{\sigma} \gamma - (\gamma-1)}} \quad (19)$$

Eqs.(18) and (19) then simplify to

$$\hat{\gamma} = \frac{\xi}{\sigma} \gamma \phi^2, \quad \hat{a} = \bar{a} \phi, \quad \hat{M} = \frac{\hat{u}}{\hat{a}} = \frac{\bar{u}}{\bar{a} \phi} = \frac{\bar{M}}{\phi} \quad (20)$$

The distributions of flow properties over the section 1 are given in advance, but the distributions at the section 2 of the shock are not known and their computation would be a troublesome and time-consuming problem. This difficulty can be avoided by assuming that the distributions of velocity and density on the two sections are similar. This assumption should be an acceptable approximation for relatively weak shock waves.

It follows from the assumption of similarity of profiles ahead and behind the wave that each of the shape factors has the same value on the two sections of the control volume:

$$\sigma_1 = \sigma_2, \quad \xi_1 = \xi_2 = \xi$$

$$\hat{\rho}_1 \hat{u}_1 = \hat{\rho}_2 \hat{u}_2 \quad (21)$$

$$\hat{p}_1 + \hat{\rho}_1 \hat{u}_1^2 = \hat{p}_2 + \hat{\rho}_2 \hat{u}_2^2 \quad (22)$$

$$\hat{\gamma} \frac{\hat{p}_1}{\hat{\rho}_1} + \frac{\hat{\gamma}-1}{2} \hat{u}_1^2 = \hat{\gamma} \frac{\hat{p}_2}{\hat{\rho}_2} + \frac{\hat{\gamma}-1}{2} \hat{u}_2^2 \quad (23)$$

Eqs. (21)~(23) are the same as the usual one-dimensional flow forms across a normal shock wave. Therefore, the Mach number just ahead of the shock wave can be obtained from the well-known expression connecting the shock Mach number to the pressure ratio across a normal shock.

$$\hat{M}_1^2 = \frac{\hat{\gamma}-1}{2\hat{\gamma}} \left( \frac{\hat{p}_2}{\hat{p}_1} - 1 \right) + 1 \quad (24)$$

## 2.4 Choking Criteria

An important limit is the shock wave of vanishing strength. i.e., an acoustic wave, obtained by setting the pressure ratio in Eq.(24) to unity. The result yields the approach Mach number required to keep an acoustic wave stationary:

$$\hat{M}_1 = 1 \quad (25)$$

It should be noted that the choking criteria with the known velocity profile at the nozzle exit can be explicitly found. It is noted that the concept of flow choking at Mach one is no longer valid in the present analysis. Indeed, when nozzle flow is choked, the individual freestream Mach numbers at the nozzle exit plane will not be equal to unity<sup>[4][5]</sup>.

## 3 Experimental Setup

Experiments were conducted in a continuous type indraft wind tunnel as shown in Fig.2. The wind tunnel consists primarily of a convergent nozzle of a variable length from the inlet to exit, settling chamber with a volume of 0.35 m<sup>3</sup>, vacuum pump, and silencer.

Four types of convergent nozzles were investigated as the test nozzles and the nozzle shape is schematically shown in Fig.3. The convergent nozzle is composed of a convergent part and straight pipe. The straight pipe has an inner diameter of  $D = 15$  mm and a length of  $L = 113$  mm ( $L/D = 7.5$ ), 150 mm ( $L/D = 10$ ), 300 mm ( $L/D = 20$ ), and 450 mm ( $L/D = 30$ ). Increases in length of the straight pipe lead to increases in the boundary layer thickness at the

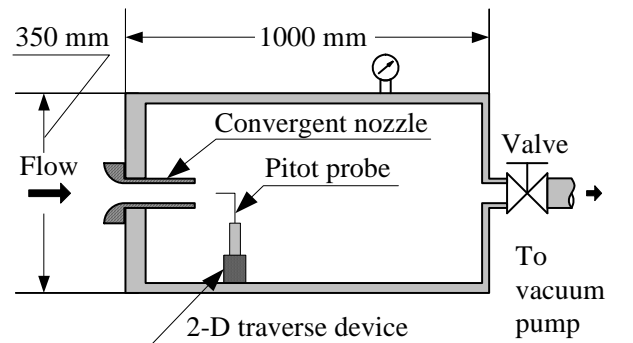


Figure 2. Schematic drawing of indraft supersonic wind tunnel

**THEORETICAL AND EXPERIMENTAL INVESTIGATIONS ON CHOKING PHENOMENA OF AXISYMMETRIC CONVERGENT FLOW**

nozzle exit (straight pipe exit).

The vacuum pump was placed at the downstream of the wind tunnel, and the pressure in the settling chamber (back pressure) was adjusted to a desired state by the vacuum pump before starting the experiment. The humidity of the flow was minimized by silica gel filters to avoid condensation inside the test nozzle. The pressure in the settling chamber was measured by a semiconductor pressure transducer.

Furthermore, the total pressures at the nozzle exit plane were measured using a Pitot probe with an inner diameter of 0.26 mm and an outer diameter of 0.51 mm. The Pitot probe was traversed along the cross-section of the nozzle exit in steps of 0.1 mm from the nozzle axis to the wall. When the flow issuing from the nozzle exit is supersonic, a curved shock wave forms in front of the Pitot probe. In the case, the Mach numbers are estimated from the measuring data by using the Rayleigh-Pitot tube formula.

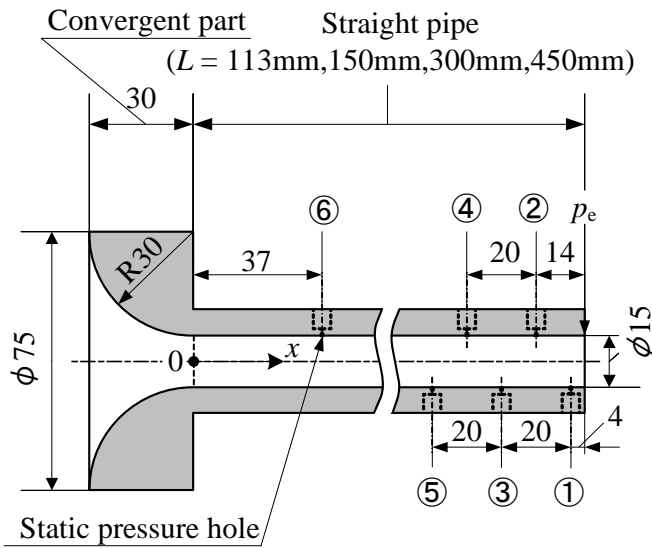


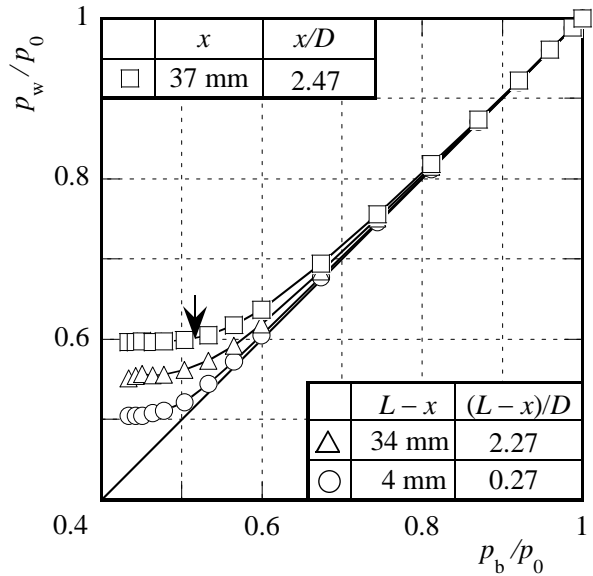
**Figure 3. Details of convergent nozzle**

**4 Results and Discussion**

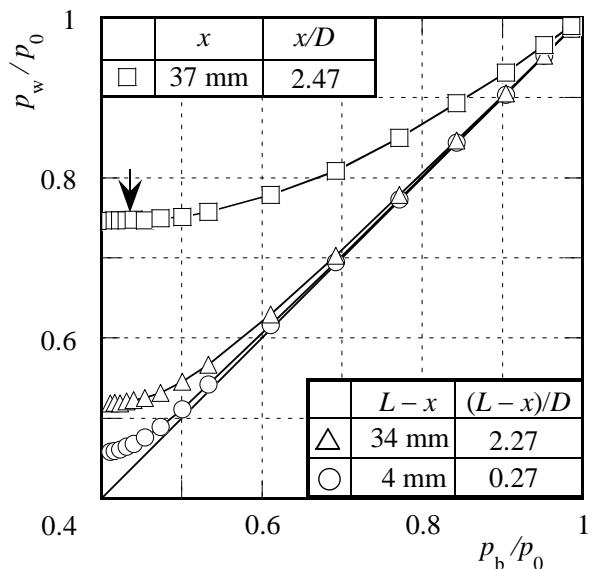
**4.1 Wall Static Pressure Distributions**

Figure 4 indicates the variation of the normalized wall pressure  $p_w/p_0$  against the ratio

$p_b/p_0$  of back pressure  $p_b$  to plenum pressure  $p_0$ . The measurements have been carried out for back pressures in a range from  $p_b = 43$  kPa to the atmospheric pressure. The circular and triangular symbols show the wall pressures for the upstream distance  $L - x = 4$  mm and 34 mm respectively from the nozzle exit and the square symbols for the downstream distance  $x = 37$  mm from the straight pipe inlet.



(a)  $L/D = 7.5$  ( $L=113$  mm)



(b)  $L/D = 30$  ( $L=450$  mm)

**Figure 4. Wall static pressure distributions**

The wall pressure  $p_w/p_0$  at the  $x = 37$  mm in Figs.4(a) and (b) initially decreases in proportion to  $p_b/p_0$  from  $p_b/p_0 = 1$  and then approaches a constant value. This means that the nozzle flow reach the choking states at a pressure ratio where changes downstream of the nozzle exit do not affect the characteristics upstream of the nozzle exit. Here, the choking pressure ratio  $(p_b/p_0)_{ch}$  is defined as the pressure ratio such that the pressure ratio becomes 0.1 % higher than the final constant value at the choking state, which is indicated by a downward-pointing arrow in Figs. 4(a) and (b). The same procedure for obtaining choking pressure ratios was repeated for the experiments for  $L/D = 10$  and 20.

It should be noted that choking criteria cannot be obtained from the wall pressure measurements near the nozzle exit because the flows there have a significant effect on the state downstream of the nozzle exit. It is obvious the fact that the wall pressure ratios near the nozzle exit decrease with a decrease in the back pressure ratio as shown by circular symbols in Fig.4.

#### 4.2 Mach Number Distributions at Nozzle Exit Plane

The local total pressures at the nozzle exit plane when the flow is just choked have been obtained using the Pitot probe on a two-dimensional traverse system. When the flow from the nozzle exit is supersonic, the Reyleigh-Pitot tube formula <sup>[8]</sup>

$$\frac{p_{0t}}{p_e} = \frac{\left(\frac{\gamma+1}{2}\right)^{\frac{\gamma-1}{\gamma+1}} M_e^{\frac{2\gamma}{\gamma-1}}}{\left(\gamma M_e^2 - \frac{\gamma-1}{2}\right)^{\frac{1}{\gamma-1}}} \quad (26)$$

is used to obtain the Mach numbers at the nozzle exit where  $p_{0t}$  is the pressure measured by a Pitot probe aimed directly against the flow direction,  $p_e$  and  $M_e$  are the static pressure and Mach number at the nozzle exit, respectively.

The results obtained are shown in Fig.5. The vertical thick line on the Mach number

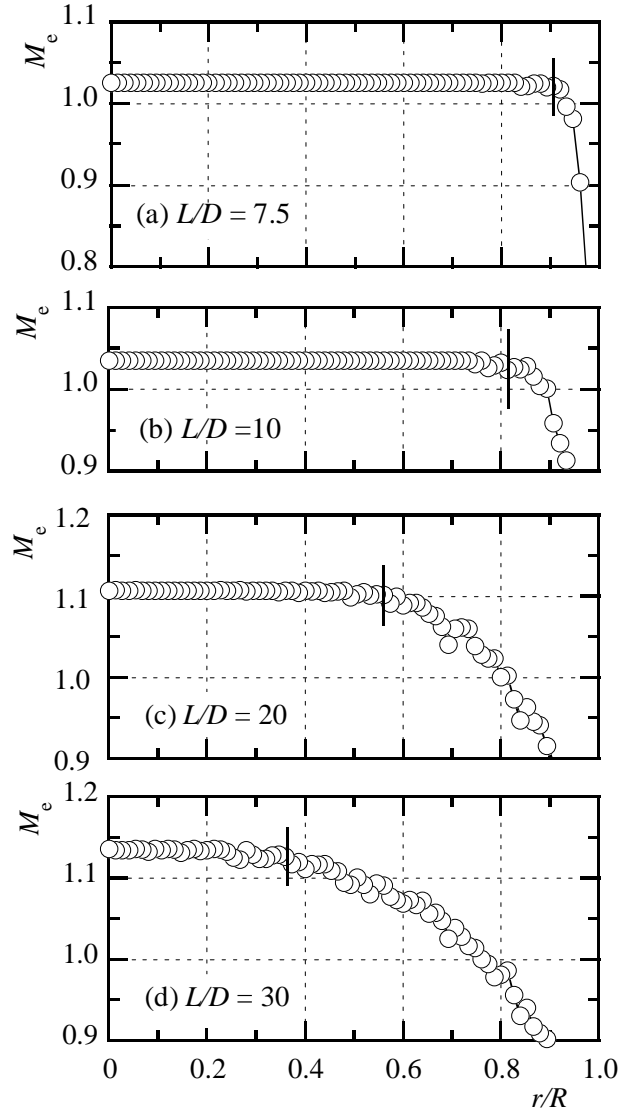


**Figure 5. Freestream Mach number distributions**

distributions in Fig.5 indicates the edge of the boundary layer.

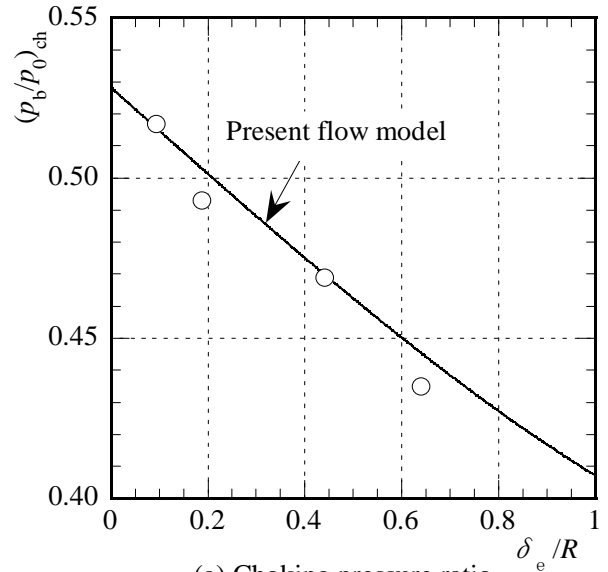
Figures 5(a)~(d) show that the freestream Mach numbers at the nozzle exit plane are larger than unity and increase with an increase in the nozzle length. Also, the boundary layer thickness at the nozzle exit increases with increasing nozzle length. In other words, when the flow is choked, an increase in boundary layer at the nozzle exit causes the freestream Mach number there to increase and the freestream Mach number is always beyond unity.

It should be noted from Fig.5(d) in particular that the nozzle flow is choked despite the flow includes a large amount of subsonic regions. This confliction can be removed by introducing a concept of compound waves<sup>[4]</sup> that disturbances cannot propagate at different absolute velocities in each stream without violating the condition that the static pressures at the stream interfaces be equal. Therefore, the disturbances must be continuous and must travel as a single wave. This means that flow disturbances propagating through the fluid as pressure waves are not traveling at the usual speed of sound but at different speed as compound waves. Bernstein et al.<sup>[4]</sup> proposed a concept of a compound wave for the choking phenomena of one or more gas streams flowing through a single nozzle with assumptions that the flow in each stream is steady, adiabatic, and isentropic. In their hypothesis, any changes in flow conditions downstream of the throat are transferred as compound waves. However, the compound flow model of Bernstein et al. does not take into account the effect of the nonuniform velocity profile caused by the boundary layers on flow choking because their model doesn't contain the influence of flow mixing inside of the boundary layers. Therefore, flow choking phenomena for the present experiments cannot be explained by the model of Bernstein et al.

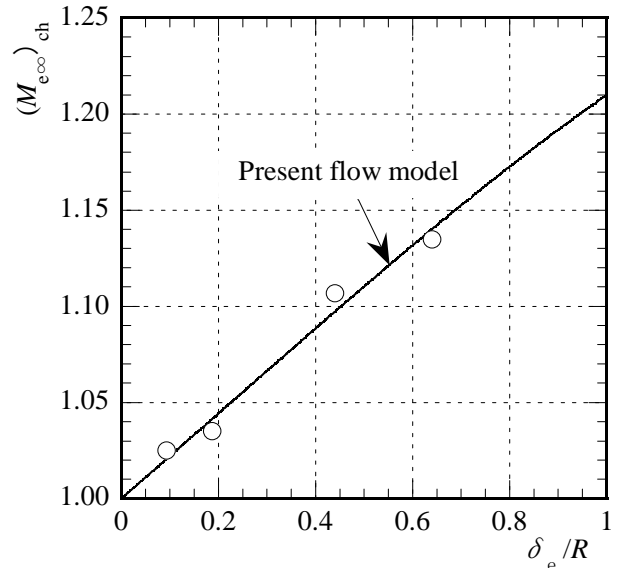
**4.3 Choking Criteria of Convergent Nozzle Flow**

Figure 6 shows choking criteria of convergent nozzle flows. Open symbols and solid line in Fig.6 indicate the present experimental data and flow model proposed. The abscissa is the boundary layer relative thickness characterized as the ratio of the boundary thickness at the nozzle exit to the pipe radius.

The value on the vertical axis for  $\delta_e / R = 0$  in Figs.6 (a) and (b) coincide with the choking criteria by the inviscid theory. The values of the choking pressure ratio calculated by the present flow model are lower than those of the inviscid theory and monotonically decrease with an increase in the wall boundary layer thickness. The calculated results are in



(a) Choking pressure ratio



(b) Freestream Mach number at nozzle exit

**Figure 6. Choking Criteria of Convergent Nozzle Flows**

good quantitative agreements with the present experimental data. Choking criteria for flow through a convergent nozzle with a nonuniform velocity distribution at the exit are that Mach number at the nozzle exit calculated by the present flow model becomes unity.

**5 Conclusions**

Effects of boundary layers at the nozzle exit on the choking phenomena of convergent nozzle flows have been demonstrated theoretically and

experimentally. A simple flow model for predicting the choking criteria of convergent nozzle flows were proposed using a mass-weighted averaging technique.

The choking pressure ratio defined as the ratio of back pressure to plenum pressure was obtained from the wall pressures at far upstream of the nozzle exit. Wall pressures near the nozzle exit are affected changes downstream of the nozzle exit even when the nozzle flow is choked.

Choking criteria can be characterized by the boundary layer thickness at the nozzle to the duct radius. A comparison of theory and experiment indicates that the choking pressure ratio decreases with increasing boundary layer relative thickness. Also, the freestream Mach numbers at the nozzle exit plane are beyond unity and increase with an increase in the boundary layer relative thickness.

### Acknowledgement

This work was founded in part by Grant-in-Aid for Scientific Research (C) No.23560204 of Japan Society for the Promotion of Science. The authors thank Tatsuya Nishioka of the AISIN AW Co., Ltd. for his invaluable support to the experimental work and exceptional skills in the fabrication of the test facility.

### References

- [1] Saad M., A., *Compressible Fluid Flow*, 2nd edition, Prentice Hall, 1985, p.110.
- [2] International Organization for Standardization (ISO), (2003), Measurement of Gas Flow by Means of Critical Flow Venturi Nozzle, ISO 9300.
- [3] Nakao S., and Takamoto M., Choking Phenomena of Sonic Nozzles at Low Reynolds Numbers, *Flow Instruments and Instrumentation*, Vol.11, No.4, pp.285-291, 2000.
- [4] Bernstein A., Heiser W.H., and Hevenor C., Compound - Compressible Nozzle Flow, *Trans. of the ASME, J. Applied Mechanics*, Vol.34, No.4, pp.548-554, 1967.
- [5] Pearson H., Holliday J. B., Smith S. F., A Theory of the Cylindrical Ejector Supersonic Propelling Nozzle, *J. Royal Aeronautical Society*, Vol.62, No.574, pp.746-751, 1958.
- [6] Matsuo K., Miyazato Y., and Kim H. D., Mass-Averaging Pseudo-Shock Model in a Straight Flow

Passage, *Proceedings of the Institution of Mechanical Engineers, Part G: J. Aerospace Engineering*, Vol.213, No.6, pp.365-375, 1999.

- [7] Sajben M. Propagation of Weak Compression Waves in Nonuniform Channel Flows, *J. Propulsion and Power*, Vol.5, No.2, pp.154-157, 1989.
- [8] Emanuel, G., *Gasdynamics: Theory and Applications*, AIAA Education Series, AIAA Inc., 1986, pp.55-56.

### Copyright Statement

The authors confirm that they, and/or their company or organization, hold copyright on all of the original material included in this paper. The authors also confirm that they have obtained permission, from the copyright holder of any third party material included in this paper, to publish it as part of their paper. The authors confirm that they give permission, or have obtained permission from the copyright holder of this paper, for the publication and distribution of this paper as part of the ICAS2012 proceedings or as individual off-prints from the proceedings.